ELSEVIER

Polymer 41 (2000) 621–628

polymer

Morphological development in absorbable poly(glycolide), poly(glycolide-co-lactide) and poly(glycolide-co-caprolactone) copolymers during isothermal crystallization

Z.-G. Wang[a], B.S. Hsiao[a,*], X.-H. Zong[a], F. Yeh[a], J.J. Zhou[b], E. Dormier[b], D.D. Jamiolkowski[b]

[a]*Department of Chemistry, State University of New York at Stony Brook, Stony Brook, NY 11794-3400, USA*
[b]*Ethicon, Inc., A Johnson & Johnson Company, Somerville, NJ 08876-0151, USA*

Received 5 January 1999; received in revised form 1 March 1999; accepted 7 March 1999

Abstract

Morphological development of the homopolymer, poly(glycolide), PGA; its random copolymers, poly(glycolide-co-lactide), PGA-co-PLA (5:95 and 90:10) and segmented block copolymer, poly(glycolide-co-caprolactone), PGA-co-PCL (75:25) during isothermal crystallization was studied using simultaneous small-angle X-ray scattering (SAXS) and wide-angle X-ray diffraction (WAXD) techniques with synchrotron radiation. It was found that the lamellar morphology could best describe the superstructure of these polymers. During crystallization, both average long period (L) and lamellar thickness (l_c) exhibited notable decreases with time, which were attributed to the mechanism of secondary crystallization in the form of lamellar-stacks insertion. Both values of L and l_c were found to increase with temperature. In the chosen crystallization temperature range (100–200°C), homopolymer PGA exhibited the fastest crystallization rate and the lowest values of L and l_c, probably due to the largest degree of supercooling. As a result, in copolymers with higher content of PGA, the crystallization rate increased and the values of L and l_c decreased. The value of amorphous layer thickness (l_a) was the highest in PGA-co-PLA (5:95), but those in PGA, PGA-co-PLA (90:10) and PGA-co-PCL (75:25) were about the same. In addition, the values of L, l_c and the crystallinity were the highest in PGA-co-PLA (5:95). Corresponding degrees of crystallinity in PGA homopolymer and PGA-co-PCL (75:25) and PGA-co-PLA (90:10) copolymers were relatively low.

Keywords: Crystallization; Lamellar morphology; Absorbable

1. Introduction

Biodegradable aliphatic polyesters can be categorized into four different groups based on their chemical structure: poly(α-hydroxy alkanoate)s; poly(β-hydroxy alkanoate)s; poly(ω-hydroxy alkanoate)s; and poly(alkylene dicarboxylate)s. Their synthesis, and thermal and physical properties are intrinsically different and depend on the chemical structure [1]. However, it is well known that the biodegradation behavior is strongly affected by the solid-state crystalline property of the polyesters [1,2]. Certainly, this is the case of poly(glycolide) (PGA), and poly(lactide) (PLA), which are all well-known bioabsorbable and biocompatible crystalline polymers [3]. Many investigations have been made to understand the degradation behavior of these polymers during in vitro and in vivo biochemical applications [4–12]. In these studies, it was evident that it is the degree of crystallinity and molecular orientation that dominate the degradation behavior. For example, the rate of enzymatic degradation of PCL fibers was found to be dependent on the draw ratio, indicating that crystallinity and crystal orientation have a role in biodegradability by lipase [1]. The study of degradation in films of butylene succinate–ethylene succinate copolymer indicated that the degradation rate is also dependent on the degree of crystallinity [1].

However, our current understanding of polymer crystallization suggests that in addition to crystallinity, the issue of polymer morphology must also play an important role to determine the degradation properties. As the biodegradation mechanism for aliphatic polyesters usually follows the hydrolysis route (such as enzymatic hydrolysis, via lipases or PHA depolymerases), the arrangement of crystal and amorphous phases should determine how the degradation process can initiate and proceed. The problem of diffusion of small molecules such as water in the biodegredable polymer medium has been well documented [10].

We believe that the crystalline morphology in the sample

* Corresponding author. Tel.: +1-516-632-7793; fax: +1-516-632-6518.
E-mail address: bhsiao@notes.cc.sunysb.edu (B.S. Hsiao)

0032-3861/00/$ - see front matter
PII: S0032-3861(99)00200-1

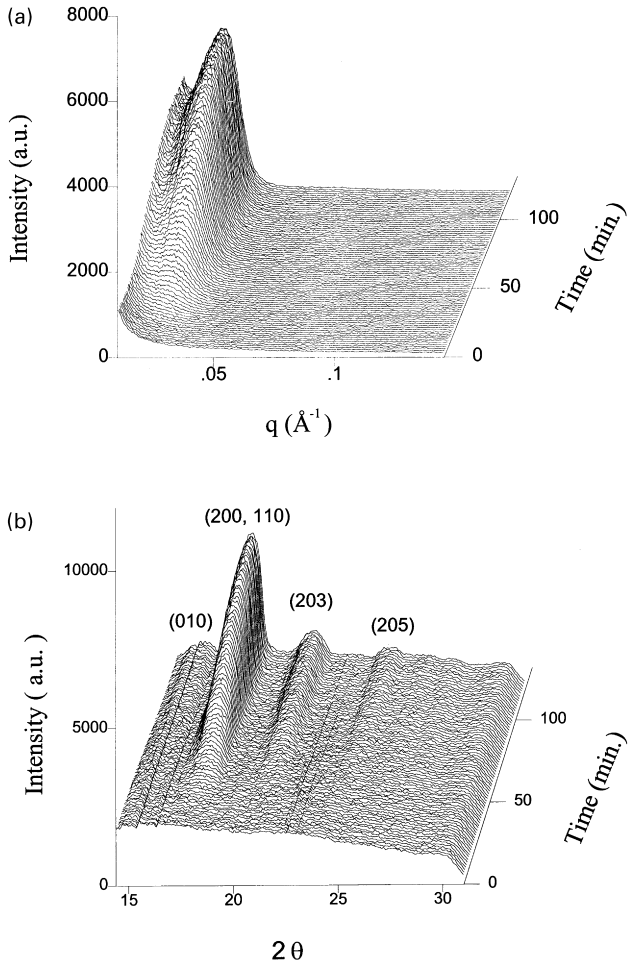

Fig. 1. Time-resolved (a) SAXS and (b) WAXD profiles during isothermal crystallization process of PGA-co-PLA (5:95) at 140°C.

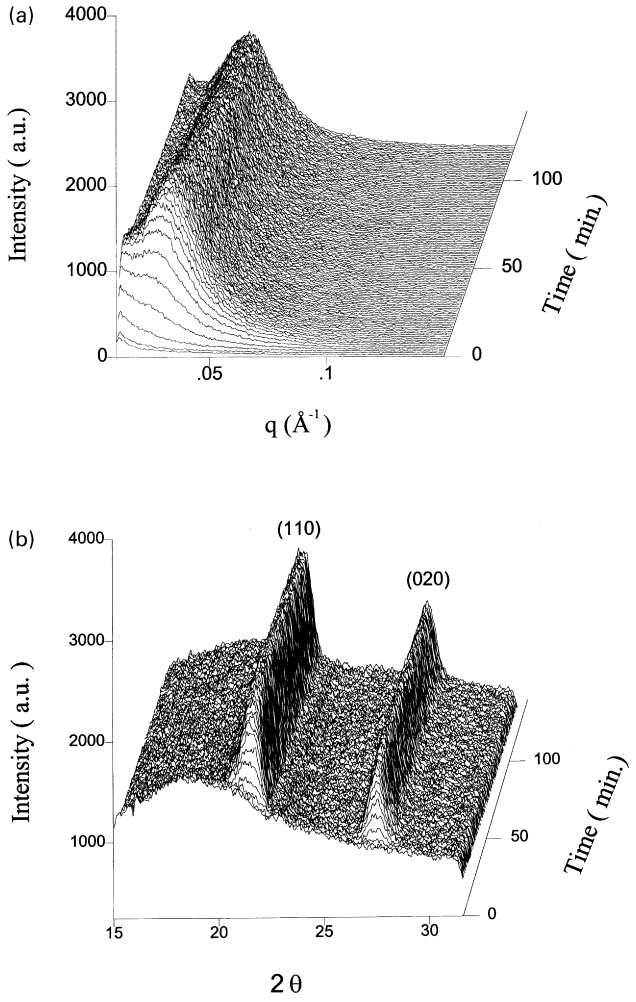

Fig. 2. Time-resolved (a) SAXS and (b) WAXD profiles during isothermal crystallization process of PGA-co-PLA (90:10) at 180°C.

is much more complicated than the overall level of crystallinity. The crystalline morphology is a strong function of the crystallizing environment, e.g. under quiescent or flow conditions. Perhaps, the lack of understanding in the relationship between the morphology and degradation mechanism has limited our ability to control the degradation properties of the final product. Thus, this study represents our first attempt to understand the development of crystal morphology and crystallinity during isothermal crystallization of bioabsorbable crystalline polymers. In future, we plan to probe the effect of flow or molecular orientation on the crystallization behavior of these polymers. To follow the rapid structure changes during crystallization, we have adopted the simultaneous small-angle X-ray scattering (SAXS) and wide-angle X-ray diffraction (WAXD) techniques with synchrotron radiation, which has only become available recently [13].

In this study, the chosen polymer system was based on the PGA homopolymer, certain random copolymers and a segmented block copolymer. The random copolymers were poly(glycolide-co-lactide) (PGA-co-PLA), and the segmented block copolymer was poly(glycolide-co-caprolactone) (PGA-co-PCL). These polymers are the basic resins for surgical products such as Vicryl* and Monocryl* sutures [14]. The crystalline structures of PGA, PLA, PCL and the stereocomplex of enantiometric PLA (PLLA and PDLA) have been determined by X-ray diffraction, electron microscopy and molecular modeling [15–21]. Extensive studies have been made to characterize the crystallization kinetics of PLA, PGA, PCL or their copolymers using differential scanning calorimetry (DSC) and optical microscopy [22–26], but still not much is known about the development of the morphological parameters such as lamellar crystal thickness and interlamellar amorphous thickness. The latter may be particularly important to the degradation process by hydrolysis.

2. Experimental

Two PGA-co-PLA random copolymers and one PGA-co-PCL segmented copolymer were used in this study. The first PGA-co-PLA copolymer contained 5% glycolide acid and

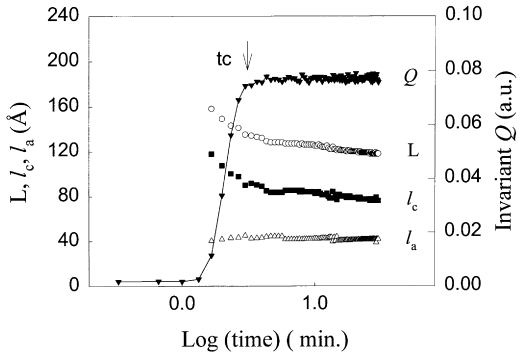

Fig. 3. Time evolution of the invariant, Q, long period, L, lamellar thickness, l_c, and amorphous layer thickness, l_a, during isothermal melt crystallization of PGA at 200°C.

95% L-lactide acid, which had an inherent viscosity of 1.52 dl/g. The second PGA-co-PLA copolymer contained of 90% glycolide acid and 10% L-lactide acid, with an inherent viscosity of 1.60 dl/g. The inherent viscosity was measured in a solution of hexafluorisopropanol (HFIP) with the polymer concentration of 0.1 g/dl at 25 °C. Both were random copolymers as confirmed by NMR spectroscopy. The melting temperatures of PGA-co-PLA (5:95) and PGA-co-PLA (90:10) were 173 and 201°C, respectively. The PGA-co-PCL segmented block copolymer contained 75% glycolide acid and 25% caprolactone, with a melting temperature of 217°C. The blocky nature was due to the multiple steps used during polymerization, and also confirmed by NMR. The weight average molecular weight (M_w) of these copolymers was about 80 000 g/mol with a polydispersity about 2. For comparison purposes, the PGA homopolymer (M_w about 60 000 g/mol) was also studied. PGA had a melting temperature of 220°C. The melting temperatures of these polymers were measured by DSC with a heating rate of 20°C/min.

The simultaneous SAXS and WAXD experiments were carried out at the X27C beamline in the National Synchrotron Light Source (NSLS), Brookhaven National Laboratory (BNL). X-rays were focused with a three-pinhole collimator [13]. The wavelength λ used was 1.307 Å. Two linear position sensitive detectors (MBraun) connected in series

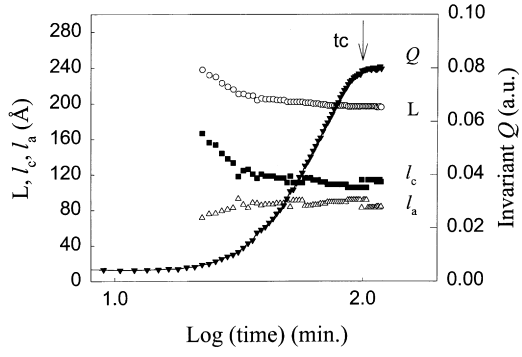

Fig. 4. Time evolution of Q, L, l_c, and l_a during isothermal melt crystallization PGA-co-PLA (5:95) at 140°C.

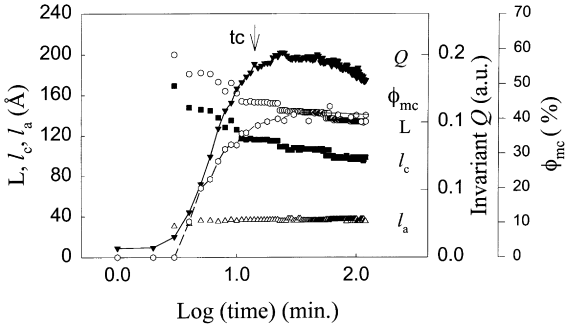

Fig. 5. Time evolution of Q, L, l_c, l_a and crystallinity ϕ_{ms} during isothermal melt crystallization of PGA-co-PLA (90:10) at 180°C.

were used to record the simultaneous SAXS and WAXD profiles. The chosen data collection times per frame were 10, 20, 60 or 90 s, respectively (depending on the crystallization rate). An evacuated flight path was used for the SAXS detection (sample to detector distance was 1190 mm). The WAXD detector covered an angular range from $12° < 2\theta < 32°$, which was sufficient to observe the strong crystal reflections from the copolymers.

A dual chamber temperature jump apparatus was used for the isothermal crystallization study. The detailed description of this apparatus has been provided previously [27,28]. Briefly, the samples were melted at a temperature (T_1) above the melting point for 5 min in one chamber and then pneumatically "jumped" to the second chamber at a lower temperature (T_2) for the measurement of crystallization. The values of T_1 were 230°C for PGA, 225°C for the copolymers. The estimated time for temperature equilibration after the jump was about 90 s, although the initial 90% of the temperature change had a rate of about 300°C/s. Upon thermal equilibration, the temperature fluctuations were less than ±0.2°C. The second chamber maintained at the crystallization temperature ($T_2 = T_c$) was aligned with the path of the X-ray beam.

The SAXS data was analyzed via the method of correlation function $\gamma(r)$ for semicrystalline polymers. The theory of this approach can be found in a previous paper [29]. With this method (after determining the Porod parameters and correcting the liquid scattering and finite interface between

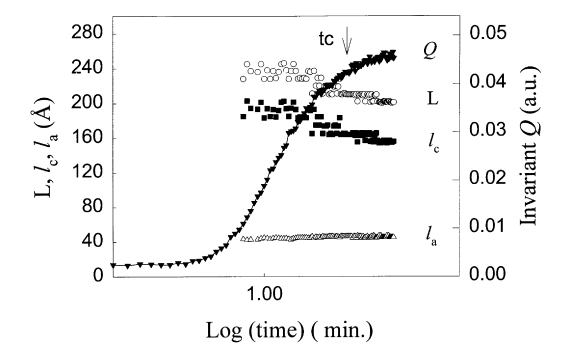

Fig. 6. Time evolution of Q, L, l_c, and l_a during isothermal melt crystallization of of PGA-co-PCL (75:25) at 190°C.

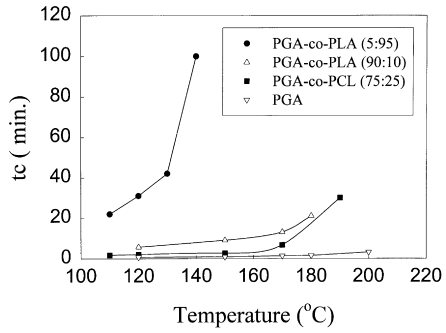

Fig. 7. The value of t_c as a function of crystallization temperature for PGA homopolymer and copolymers.

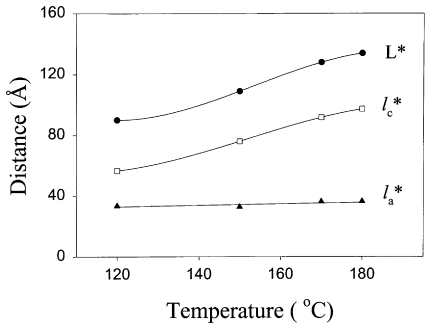

Fig. 9. The changes of L^*, l_c^* and l_a^* at different crystallization temperature for PGA-co-PLA (90:10) copolymer.

the scattering phases), we can calculate several morphological variables including long period L, lamellar thickness l_c, amorphous layer thickness l_a, and the scattering invariant Q, assuming that the system follows a two-phase lamellar stacks model. For the WAXD data, the integrated intensities, peak positions, peak heights and peak widths for crystal reflection peaks and amorphous background were calculated by a deconvolution method (all peaks were chosen to be Gaussian) using the program GRAMS/32 Spectral Notebase™ (Galactic Industries Corporation). In this study, two Gaussian peaks were used to fit the amorphous phase, which does not have the shape of a single curve function. By dividing the total intensities of the crystalline reflections I_c to the overall intensity I_{total}, a measure of the mass fraction of the crystalline phase in the sample can be obtained. This value is termed as the apparent mass degree of crystallinity, ϕ_{mc}. Owing to the possible distortions in the crystal lattice and thermal disorder, the measured value of I_c might underestimate the true value of crystallinity. The mass crystallinity is related to the volume degree of crystallinity, ϕ_{vc}, as $\phi_{mc} = f(T)\ \phi_{vc}$, where $f(T)$ is a temperature-dependent factor taking into account of the deviations mentioned above and the conversion from mass to volume.

3. Results and discussion

Figs. 1 and 2 show typical simultaneous SAXS (I versus q, where $q = (4\pi/\lambda)\ sin(\theta)$) and WAXD ($I$ versus 2θ) profiles in real time during isothermal crystallization of PGA-co-PLA (5:95) at 140°C and PGA-co-PLA (90:10) at 180°C, respectively. From SAXS profiles, it is seen that in the initial induction period, all scattering curves are diffuse (without scattering maximum). After the induction period, a clear scattering maximum is seen, which progressively shifts to higher scattering angles. These changes are accompanied by an increase in the scattering intensity. Corresponding WAXD profiles in Figs. 1b and 2b indicate that the crystal structures of the two PGA-co-PLA copolymers, 5:95 and 90:10, are very different, and they resemble the homopolymers of PLA [30] and PGA [17], respectively. Both PLA and PGA crystals are found to be an orthorhombic unit cell. The indices of the major reflections are marked in Figs. 1(b) and 2(b), respectively. We have compared the unit cell parameters of the PGA homopolymer and the PGA-co-PLA (90:10) copolymer and found that no expansion of the cell dimensions can be seen. This suggests that glycolate and lactate probably do not cocrystallize, and the low concentration of the component in the copolymers remains largely amorphous. However, we are not certain if the copolymer moieties are completely or partially segregated at the lamellar surface.

With the method of correlation function [29], morphological parameters such as the scattering invariant (Q), the average long period (L), lamellar thickness (l_c) and amorphous interlayer thickness (l_a), can be extracted from the

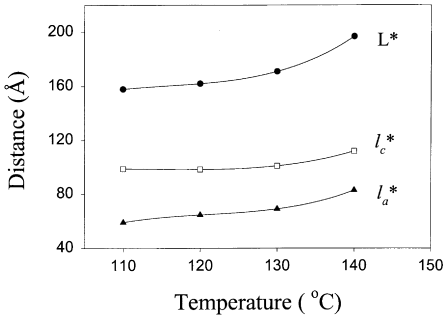

Fig. 8. The changes of L^*, l_c^* and l_a^* at different crystallization temperature for PGA-co-PLA (5:95) copolymer.

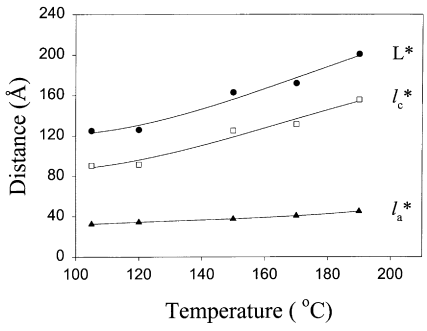

Fig. 10. The changes of L^*, l_c^* and l_a^* at different crystallization temperature for PGA-co-PCL (75:25) copolymer.

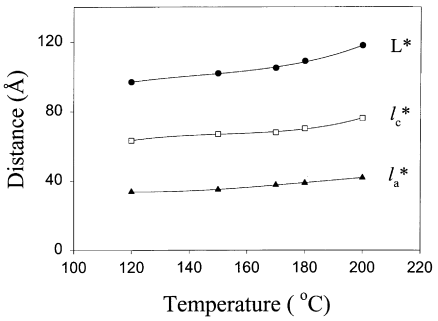

Fig. 11. The changes of L^*, l_c^* and l_a^* at different crystallization temperature for PGA homopolymer.

SAXS data. As the correlation function method only gives rise to values of two average thicknesses in the two-phase lamellar model (l_1 and l_2), we have assigned the larger value l_1 as the lamellar thickness l_c and the lower value l_2 as the amorphous layer thickness l_a. The reason for this assignment will be discussed later. Evolution of the morphological parameters (Q, L, l_c, l_a) in the homopolymer PGA (at 200°C), random copolymers PGA-co-PLA (5:95) (at 140°C) and PGA-co-PLA (90:10) (at 180°C), and segmented copolymer PGA-co-PCL (75:25) (at 190°C) during isothermal crystallization are depicted in Figs. 3–6, respectively. In Fig. 5, the evolution of crystallinity from WAXD curves is also included.

Three common features in the morphological variables during isothermal crystallization of these polymers can be identified. (1) The invariant Q exhibits a sigmoidal increase with log time. During the primary crystallization dominant stage (less than t_c, which is defined as the characteristic time to complete the primary crystallization), the average long period (L) and the average lamellar thickness (l_c) exhibit a significant decrease. Similar observations have also been reported previously in other polymers such as poly(ether-etherketone), PEEK, and poly(ethylene terephthalate), PET [27,29,31]. In these polymers, calorimetric studies indicate that this regime corresponds to the development of the major endotherm [32,33]. (2) During the secondary crystallization dominant stage (greater than t_c), L and l_c exhibit a small decay. (3) The change in the interlamellar amorphous layer thickness (l_a) is significantly less than the changes in L and l_c. We can attribute these features to the secondary crystallization process, probably in the form of lamellar stack insertion. As secondary crystallization occurs with the formation of thinner defective lamellar stacks between the existing primary stacks (with larger thickness), this will result in a significant decrease in L and l_c, and a slight increase in l_a, which has been well documented in other polymers [27–31,33–35].

In this study, the SAXS and WAXD signals were measured simultaneously, the comparison of the kinetics from each signal can be made to reveal the nature of initial crystallization. It is thought that if the SAXS signal occurs prior to the crystalline reflections in WAXD, the event of

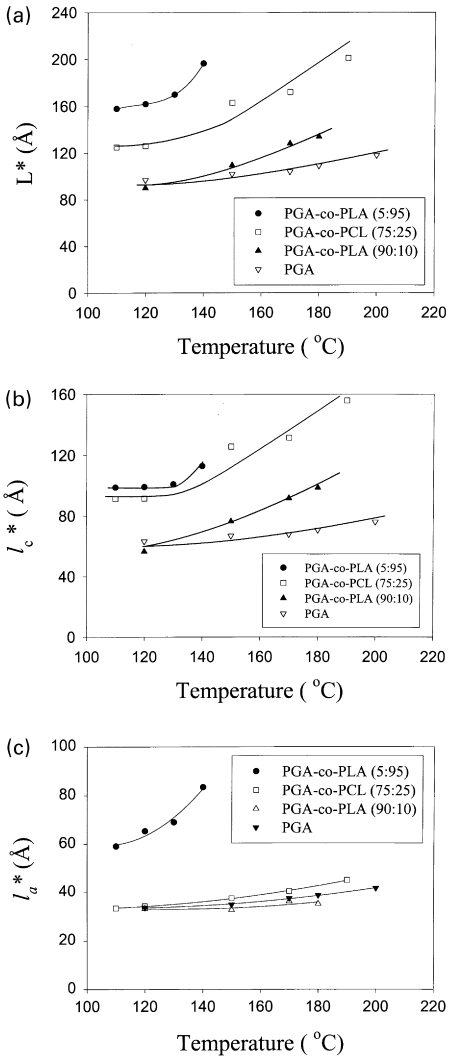

Fig. 12. Comparison of (a) long period L^* (b) lamellar thickness l_c^* and (c) amorphous layer thickness l_a^* at different temperatures between PGA copolymers and PGA homopolymer.

density fluctuations (which manifest in SAXS) may serve as a precursor to crystallization (the ordering manifests in WAXD). This behavior has been observed during the crystallization of PET [36] and poly(etherketoneketone), PEKK [37]. However, in this study, there appears to be no discrepancy between the SAXS and WAXD signals. This can be seen in Fig. 5 with the comparison of Q and ϕ_{mc}, which occur almost simultaneously.

The variation of t_c (defined as the onset time to reach the plateau Q value) is shown in Fig. 7. The value of t_c always increases with increasing temperatures as expected due to the lowering degree of supercooling (the difference between the crystallization temperature and the melting point). However, we found that the observed value of t_c at a chosen crystallization temperature has the following order: PGA-co-PLA (5:95) > PGA-co-PLA (90:10) > PGA-co-PCL (75:25) > PGA. This indicates that PGA has the fastest isothermal crystallization rate. The PGA-co-PCL (75:25)

Table 1
Morphological parameters: L^*; l_c^*; l_a^* and ϕ_{mc}, the primary crystallization characteristic time, t_c and isothermal crystallization time, t_{iso} for varying PGA homopolymer and copolymers

T (°C)	l_a (Å)	l_c (Å)	L (Å)	ϕ_m (%)	t_c(min)	t_{iso}(min)
PGA homopolymer						
120	33.7	63.3	97.0	0.34	0.67	15
150	35.0	67.0	102.0	0.35	0.83	20
170	37.6	67.9	105.5	0.35	1.3	30
180	38.8	70.2	109.0	0.36	1.5	40
200	41.8	76.2	118.0	0.40	3.1	30
PGA-co-PLA (5:95) copolymer						
110	59.1	98.9	158.0	0.40	22	40
120	64.6	98.4	163.0	0.40	31	60
130	69.0	101.0	170.0	0.43	42	120
140	83.0	112.0	195.0	0.47	100	120
PGA-co-PLA (90:10) copolymer						
120	33.4	56.6	90.0	0.37	5.7	20
150	33.0	76.0	109.0	0.40	9.0	30
170	36.3	91.7	128.0	0.41	13	60
180	36.7	97.3	134.0	0.41	21	120
PGA-co-PCL (75:25) copolymer						
110	34.5	90.5	125.0	0.27	1.7	27
120	34.4	91.6	126.0	0.26	2.0	20
150	38.0	125.0	163.0	0.27	2.7	27
170	40.6	131.4	172.0	0.29	6.7	27
190	45.1	155.9	201.0	0.30	30	40

segmented copolymer has a faster crystallization rate than the random copolymers of PGA-co-PLA (5:95) and PGA-co-PLA (90:10), which is consistent with the blocky sequence of the PGA moiety in the chain. The slowest rate of PGA-co-PLA (5:95) is due to the dominant PLA components and the corresponding lower degrees of supercooling in PLA (its nominal melting point is only about 168°C, compared with 220°C for pure PGA).

Above the characteristic time t_c, the values of L, l_c and l_a reach the plateau level, and the plateau values (indicated by the asterisk symbol) at different temperatures are shown in Figs. 8–11, which correspond to random copolymers PGA-co-PLA (5:95) and PGA-co-PLA (90:10), segmented block copolymer PGA-co-PCL (75:25), and homopolymer PGA. It can be seen that the values of L^* and l_c^* increase notably with the crystallization temperature in these figures. The corresponding interlamellar amorphous layer thickness (l_a^*) also shows a slight increase in PGA-co-PLA (90:10), PGA-co-PCL (75:25) and PGA (Figs. 9–11), while it remains almost constant in PGA-co-PLA (5:95) (Fig. 8). The values of L^*, l_c^* and l_a^* are compared among the different polymers as shown in Fig. 12(a)–(c). It is seen that homopolymer PGA has the lowest values of L^* and l_c^*, which increase slightly with temperature. This is consistent with the lowest values of t_c in PGA. As its crystallization rate is fast (the degree of supercooling is high), the resultant crystal structure can be quite defective. In PGA dominant copolymers (PGA-co-PLA (90:10) and PGA-co-PCL (75:25)), the decrease of the PGA content increases L^* as well as l_c^*, whereas the values of the amorphous layer thickness in PGA, PGA-co-PLA (90:10) and PGA-co-PCL (75:25) are very close. In the PLA dominant copolymer PGA-co-PLA (5:95), it is seen that the values of L^*, l_c^* and l_a^* are the highest among the four polymers. This can be attributed to the lower degrees of supercooling for PLA at the chosen crystallization temperatures. For the purpose of comparison, all morphological variables from different polymers are summarized in Table 1.

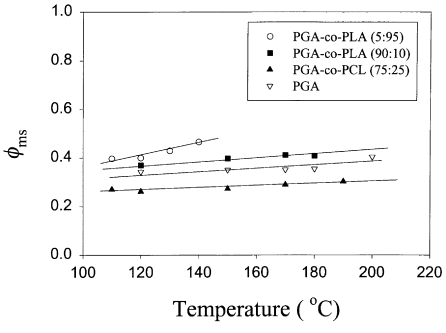

Fig. 13. Comparison of the degree of crystallinity (ϕ_{mc}) from WAXD data at different temperatures between PGA copolymers and PGA homopolymer.

From the WAXD data, the mass degree of crystallinity, ϕ_{mc}, has also been calculated and the plateau crystallinity (at time $>t_c$) of the different polymers is shown in Fig. 13. It is seen that copolymer PGA-co-PLA (5:95) has the highest degree of crystallinity (40–50%), which is in agreement with the values published before [38] as well as with the report that PLA homopolymer has a maximum degree of crystallinity about 60% (by DSC) [39]. Copolymer PGA-co-PCL (75:25) has the lowest values of degree of crystallinity, in spite of a low value of t_c and high values of L^* and l_c^*. The degrees of crystallinity of homopolymer PGA and copolymer PGA-co-PLA (90:10) lie between PGA-co-PCL (75:25) and PGA-co-PLA (5:95). The slightly higher crystallinity in PGA-co-PLA (90:10) than PGA is due to the relatively longer crystallization time t_{iso} used during the measurement of PGA-co-PLA (90:10) copolymer.

With the use of combined WAXD and SAXS results, we can verify that the assignment of l_1 as the lamellar thickness l_c is correct. Our reasons are as follows. In PGA homo- and co-polymers, as their degrees of crystallinity are relatively low, one may consider the low value, l_2, to be the lamellar thickness. However, this turns out to be not the case for the following reasons. If we define the ratio l_1/L or l_2/L as the possible linear degree of crystallinity for the lamellar stacks. The volume-filling fraction of the lamellar stacks, Xs, times this linear degree of crystallinity in lamellar stacks should be equal to the volume degree of crystallinity ϕ_{vc}. Here we can approximate the value of ϕ_{vc} to be about the same as the mass degree of crystallinity ϕ_{mc}, because the difference between the density of amorphous PGA ($\sim$1.50 g/cm^3) and the 100% crystalline PGA ($\sim$1.70 g/cm^3) is small [40]. The calculated values for Xs are shown in Fig. 14 (a)–(d). From these figures, it is clear that if l_2 is assigned

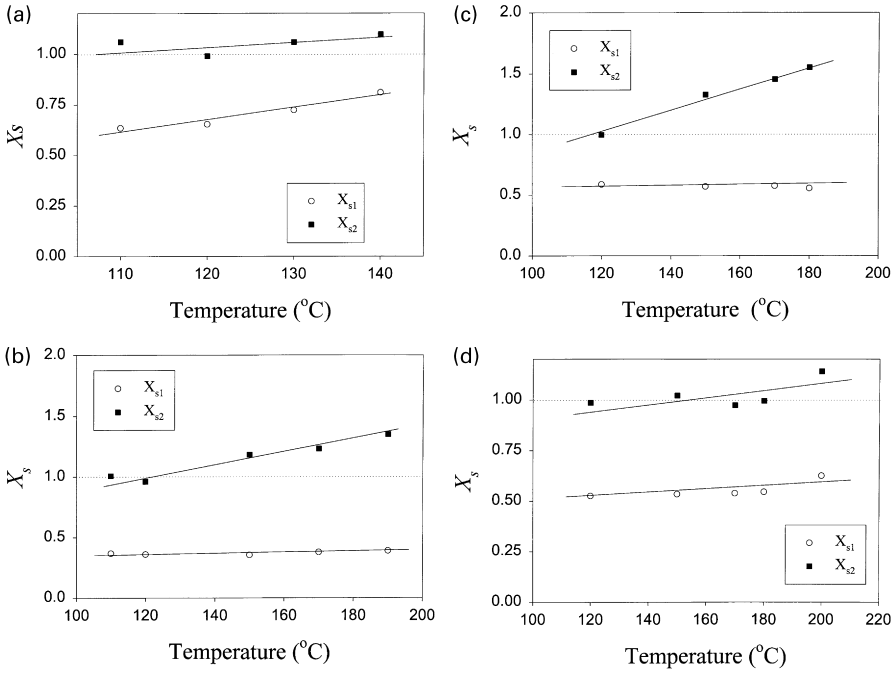

Fig. 14. Volume-filling lamellar stacks fraction, *X*s, at different temperatures for copolymers (a) PGA-co-PLA (5:95) (b) PGA-co-PLA (90:10) (c) PGA-co-PCL (75:25), and homopolymer (d) PGA.

as the lamellar thickness, the volume-filling fraction Xs_2 will be larger than unity at high crystallization temperatures or near unity at low crystallization temperatures for PGA homo- and co-polymers, which cannot be physically meaningful. As a result, the l_1 should represent l_c, and the volume-filling fraction Xs_1 should lie between 40 and 75% for these polymers. This indicates that large domains of amorphous phase probably exist between the lamellar stacks. These domains may consist of chain ends, entanglement, excluded minor components that are most susceptive to the hydrolysis process. We will attempt to correlate the degradation properties with the lamellar morphology in a future paper.

4. Conclusion

During isothermal crystallization of PGA and its copolymers (random and segmented), we found that both values of average long period (L) and lamellar thickness (l_c) exhibit a decrease with time. This behavior can be explained by secondary crystallization probably in the form of lamellar stack insertion. The pure PGA material shows the fastest crystallization rates, which is due to the largest degree of supercooling at the chosen temperature range. As a result, the decrease in the PGA content of copolymers results in the decrease in crystallization rate. The segmented copolymer PGA-co-PCL (75:25) shows a faster rate than the random copolymer PGA-co-PLA (90:10), which reflects the blocky nature of the PGA components in the segmented copolymer.

In PGA homopolymer, the values of long period and lamellar thickness are found to be the lowest and they increase slightly with temperature. In contrast, these values increase notably in copolymers, especially at high temperatures. The corresponding values of the amorphous layer thickness for PGA, PGA-co-PLA (90:10) and PGA-co-PCL (75:25) are very similar to each other. The unique behavior is seen in random copolymer PGA-co-PLA (5:95), which exhibits the largest values of L, l_c and l_a, which is attributed to the major component of PLA (having relatively small degrees of supercooling). The WAXD data supports that copolymer PGA-co-PLA (5:95) has the highest degree of crystallinity, whereas copolymer PGA-co-PCL (75:25) has the lowest and copolymer PGA-co-PLA (90:10) and homopolymer PGA have the intermediate degree of crystallinity. Finally, from the comparison of SAXS and WAXD results, we conclude that large domains of amorphous gaps exist between the lamellar stacks in PGA, PGA-co-PCL (75:25), PGA-co-PLA (90:10) and PGA-co-PLA (5:95) copolymers, which may be susceptive to the hydrolysis process.

Acknowledgements

The authors acknowledge the financial support of this work in part by a grant from NSF (DMR 9732653) and in part by Ethicon Inc.

References

[1] Mochizuki M, Hirami M. Polym Adv Technol 1997;8(4):203–209.
[2] Tsuji H, Ikada Y. J Appl Polym Sci 1997;63(7):855–863.

[3] Tighe BJ, Amass AJ, Yasin M. Macromol Symp 1997;:133–145 37th Microsymposium on Macromolecules, Biodegradable Polymers: Chemical, Biological and Environmental Aspects, 1996.
[4] MacDonald RT, McCarthy SP, Gross RA. Macromolecules 1996;29(23):7356–7361.
[5] Park A, Cima LG. J. Biomed. Mater. Res. 1996;31(1):117–130.
[6] Schugens Ch, Maquet V, Grandfils Ch, Jerome R, Teyssie Ph. J Biomed Mater Res 1996;30(4):449–461.
[7] Cordewener FW, Rozema FR, Bos RRM, Boering G. J Mater Sci: Mater Med 1995;6(4):211–217.
[8] Chu CC. J Appl Polym Sci 1981;26(5):1727–1734.
[9] Izumikawa S, Yoshioka S, Aso Y, Takeda Y. J. Controlled Release 1991;15(2):133–140.
[10] Goepferich A. Biomaterials 1997;18(5):397–403.
[11] Jamiolkowski DD, Shalaby SW. Polym Prepr (Am Chem Soc Div Polym Chem) 1990;31(2):329–330.
[12] Pistner H, Gutwald R, Ordung R, Reuther J, Muehling o. J Biomaterials 1993;14(9):671–677.
[13] Chu B, Harney P, Li Y, Linhiu K, Ye F, Hsiao B. Rev Sci Instr 1994;65(3):597.
[14] Bezwada RS, Jamiolkowski DD, Lee IY, Agarwal V, Persivale J, Trenka-Benthin S, Erneta M, Suryadevara J, Yang A, Liu S. Biomaterials 1995;16(15):1141.
[15] Dorset DL. Polymer 1997;38(2):247–253.
[16] Marega C, Marigo A, Zannetti R, Paganetto G. Eur Polym J 1992;28(12):1485–1486.
[17] Chatani Y, Suehiro K, Okita Y, Tadokoro H, Chujo K. Makromol Chem 1968;113:215–229.
[18] Cartier L, Okihara T, Lotz B. Macromolecules 1997;30(20):6313–6322.
[19] Miyata T, Masuko T. Polymer 1997;38(16):4003–4009.
[20] Thakur KM, Kean RT, Zupfer JM, Buehler NU, Doscotch MA, Munson EJ. Macromolecules 1996;29(27):8844–8851.
[21] Okihara T, Tsuji M, Kawaguchi A, Katayama K, Tsuji H, Hyon SH, Ikada Y. J Macromol Sci Phys 1991;30(1–2):119–140.
[22] Chu CC. Adv Biomater 1982;3:781–786.
[23] Grabar DG. Microscope 1970;18(3):203–213.
[24] Kolstad JJ. J Appl Polym Sci 1996;62(7):1079–1091.
[25] Chen H-L, Li L-J, Ou-Yang W-C, Hwang J C, Wong W-Y. Macromolecules 1997;30(6):1718–1722.
[26] Hoogsteen W, Postema AR, Pennings AJ, Brinke G, Zugenmaier P. Macromolecules 1990;23:634.
[27] Hsiao BS, Gardner KH, Wu DQ, Chu B. Polymer 1993;34(19):3986.
[28] Hsiao BS, Gardner KH, Wu DQ, Chu B. Polymer 1993;34(19):3996.
[29] Verma R, Marand H, Hsiao B. Macromolecules 1996;29:7767.
[30] Ikada Y, Jamshida K, Tsuji H, Hyon SH. Macromolecules 1987;20:906.
[31] Kruger K-N, Zachmann HG. Macromolecules 1993;26:5202.
[32] Cheng SZD, Cao MY, Wunderlich B. Macromolecules 1986;19:1868.
[33] Wang Z, Hsiao BS, Sauer BB, Kampert WG. Polymer 1999 in press.
[34] Verma RK, Hsiao BS. Trends Polym Sci 1996;4(9):312.
[35] Hsiao BS, Wang Z, Yeh F, Yan G, Sheth KC. Polymer 1999;40:3515.
[36] Imai M, Mori K, Mizukami T, Kaji K, Kanaya T. Polymer 1992;33:4451.
[37] Ezquerra TA, Lopez-Cabarcos E, Hsiao BS, Balta-Calleja FJ. Phys Rev E: Brief Report 1996;54(1):989.
[38] Tsuji H, Ikada Y. Polymer 1995;36:2709.
[39] Kalb B, Pennings AJ. Polymer 1980;21:607.
[40] Chujo K, Kobayashi H, Suzuki J, Tokuhara S, Tanabe M. Makromol Chem 1967;100:267.